Article Identifier
DOI: 10.22032/dbt.58860
URN: urn:nbn:de:gbv:ilm1-2023isc-037:3

60th ILMENAU SCIENTIFIC COLLOQUIUM
Technische Universität Ilmenau, 4 – 8 September 2023
URN: urn:nbn:de:gbv:ilm1-2023isc:1

CAPTURING 3D TEXTURED INNER PIPE SURFACES FOR SEWER INSPECTION

Darko Vehar, Rico Nestler, Karl-Heinz Franke

Zentrum für Bild- und Signalverarbeitung e. V.,
Werner-von-Siemens-Str. 12, D-98693 Ilmenau
URL: www.zbs-ilmenau.de

ABSTRACT

Inspection robots equipped with TV camera technology are commonly used to detect defects in sewer systems. Currently, these defects are predominantly identified by human assessors, a process that is not only time-consuming and costly but also susceptible to errors. Furthermore, existing systems primarily offer only information from 2D imaging for damage assessment, limiting the accurate identification of certain types of damage due to the absence of 3D information. Thus, the necessary solid quantification and characterisation of damage, which is needed to evaluate remediation measures and the associated costs, is limited from the sensory side.

In this paper, we introduce an innovative system designed for acquiring multimodal image data using a camera measuring head capable of capturing both color and 3D images with high accuracy and temporal availability based on the single-shot principle. This sensor head, affixed to a carriage, continuously captures the sewer's inner wall during transit. The collected data serves as the basis for an AI-based automatic analysis of pipe damages as part of the further assessment and monitoring of sewers.

Moreover, this paper is focused on the fundamental considerations about the design of the multimodal measuring head and elaborates on some application-specific implementation details. These include data pre-processing, 3D reconstruction, registration of texture and depth images, as well as 2D-3D registration and 3D image fusion.

Index Terms **–** Snapshot-3D, sewer inspection, structured light, multimodal imaging

1. INTRODUCTION

The vast sewer network of Germany, extending approximately 550,000 kilometers, demands regular inspection and maintenance. Traditionally, tele-operated robots equipped with cameras are deployed to detect defects within these sewer systems. These inspection robots are compact due to the need to navigate pipes where over 90% have an inner diameter of 200 mm, and usually incorporate a forward-facing camera. This camera provides live or recorded visual data to an exterior monitor. Due to the fact that these systems rely heavily on human operators to identify damages, the process is subjective and dependent on the inspector’s expertise.

Despite recent advancements in AI for damage classification, automatic detection of damage in sewer sections and the creation of rehabilitation plans, are yet to be fully integrated into sewer inspection procedures. AI has demonstrated effectiveness in evaluating such omnidirectional color images [1], but is still unable to detect certain types of damage that require 3D technology for robust detection, such as deposits, sleeve offsets, root ingress, and spalling. These specific damages can reduce pipe diameter and in many cases, only rough quantitative estimates can be made by experts trough analyzing the 2D images. This necessitates a method for accurately measuring the inner walls of sewer pipes in 3D, which is the focus of this article.

1.1 Related work for 3D sewer inspection

The pioneering systems designed to capture sewer geometry and its defects utilized laser profilometry [2][3][4][5], one of the most widely used techniques for assessing the pipe geometry to this day. The process involves projecting a laser beam inside the pipe, forming a ring that is captured by an omnidirectional camera. By extracting the contour of this laser ring from the image, the cross-section of the pipe can be measured, allowing for the identification of damages through deviations from the ideal shape. Despite their simplicity and robustness, these systems are limited in the resolution of the 3D data they can provide.

3D surface models of pipes can also be generated through dense stereo matching [6][7] from an image sequence captured by a forward-facing camera. These systems typically use feature points and/or IMU to determine the camera pose for each image, and then employ passive stereo correspondence to compute the 3D model. However, this method often fails on damage-free parts of pipes due to their homogenous (non-textured) surface, which is unfavorable for passive stereo matching.

A variety of systems, like the Kinect1 or Intel RealSense, are commercially available for 3D imaging. These can be used either in a forward- [8] or downward-facing [9] configuration, on a tilting platform [10], or arranged in a convergent setup [11]. Yet, their applicability is confined to walkable sewers or larger pipe diameters due to the size of the systems and the minimum detection range of the cameras.

The only system known to use dense structured light, other than the Kinect1 sensor, was presented in [12]. This approach only examines 120° of the full 360° pipe and relies on a 4-frame phase shifting method using a static projected pattern and a moving camera. They require an inertial measurement unit to obtain precise camera positions for each captured image, which are then used to perform the 3D reconstruction. In contrast, our method robustly reconstructs the 3D surface from a single camera image of a projected structured light pattern, without additional sensor data, and allows a transverse speed of up to 100 mm/s. It should be noted that most conventional non-3D sewer inspection systems do not exceed this speed.

In this paper, we concentrate on a hardware system we have engineered for the acquisition of textured 3D images, complemented by supporting algorithms. We will highlight how innovative design decisions allow for our methods to be applied effectively in the challenging conditions found in sewer pipes. Our system creates textured 3D models of pipes with enough detail to characterize and quantify damage according to DIN-EN 13508.

2. THE DESIGN AND FUNCTION OF THE MULTIMODAL SENSOR HEAD

The multimodal sensor head is the primary feature of our approach, which incorporates camera-projector modules as depicted in Figure 1. A key component of such a module consists of a projector unit, accompanied by a 3.2-megapixel camera for capturing the sewer's surface according to the structured light principle in three dimensions (3D) as well as its colored texture.

The projector and camera units have lenses with identical focal lengths and parallel, offset imaging beam paths. We further innovated our design by introducing a custom laterally coded binary pattern [13], implemented as a photomask for projection. A power LED is utilized for projection illumination, its radiation being coupled into the projection beam path. This is achieved with a combination of a condenser, photomask, and a lens at the front. We placed additional LEDs at the front of the module to serve as a diffuse light source for capturing colored texture images of the surface.

The module is intricately engineered to accommodate a close-up range varying between a minimum of 60 mm and a maximum of 250 mm, alongside wide field angles of 76° vertically and 61° horizontally. This complex configuration imposes significant challenges on the optical design. The resulting large stereo angle of 29° provides a high depth resolution of 0.2 mm at a 200 mm diameter. As the inspection robot traverses the sewer network, it cyclically captures the data. The sensor and lighting control have been designed to ensure a substantial overlap of images in the direction of travel. This is crucial for enabling robust stitching of the individual measurements during subsequent processing stages.

The sensor head is composed of six camera-projector modules. These modules are set with a viewing direction orthogonal to the sewer pipe axis, allowing them to capture the entire measurement range (ring) at high resolution. As illustrated in Figure 2, the modules are installed in a carrier with a 150 mm outer diameter and a 600 mm length. This arrangement enables a full 360-degree 3D capture of the sewer surfaces. The entrance pupils of all modules lie on the common carrier axis which guarantees the required overlap of data fields for stitching. It is effective even when the measuring head is off-center in the sewer pipe, as well as for different sewer diameters. This practical consideration leads to our unique, axially offset spiral arrangement of the camera-projector modules.

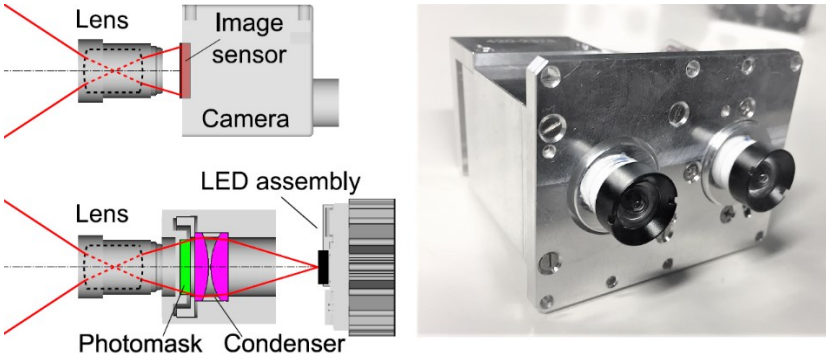

Figure 1: Schematic of the camera-projector module (left) and the finished prototype (right) for 3D surface acquisition as well as its colored texture.

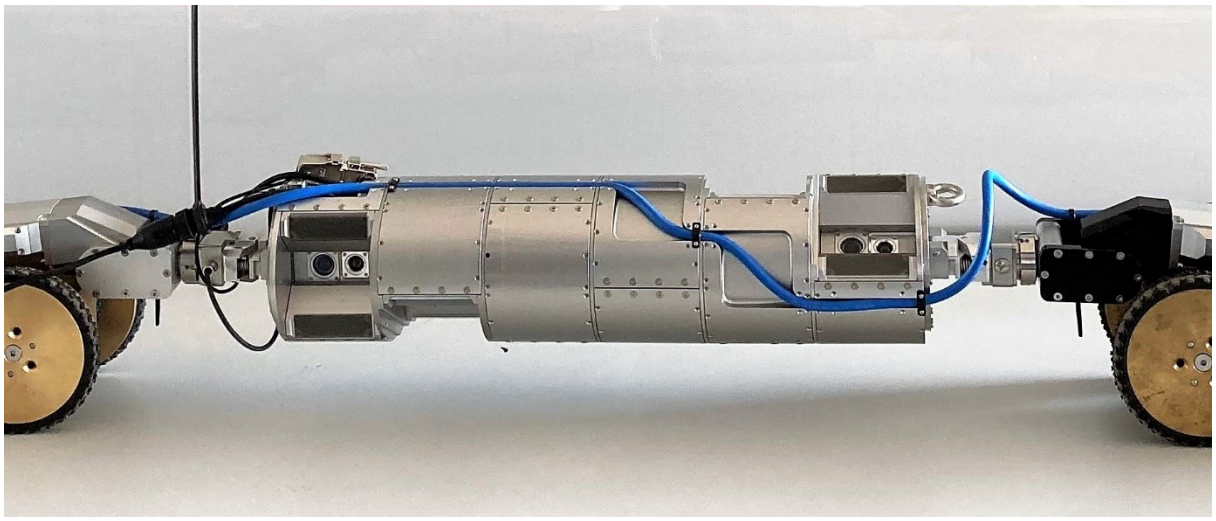

Figure 2: Sensor head with an outer diameter of 150 mm and length of 600 mm consists of six structured light modules for 360 degree capture of sewer pipes. Photo courtesy of JT-elektronik GmbH.

3. PROCESSING PIPELINE

The processing pipeline in this system involves a few challenges due to the use of a single camera in each module to sequentially capture texture and 3D imagery. Compounding this, the camera is constantly in motion throughout the sewer pipe. Therefore, a set of algorithms is required to perform a functionally essential task: capturing textured and 3D images of the pipe's inner walls during continuous capture on a moving carrier and mapping each corresponding texture to a 3D image.

3.1 Color and shading texture correction

The role of spatially-resolved detection of materials, visually represented as color or texture images, is essential for identifying significant regions and defect features in sewer lines. In this respect, chromaticity becomes a critical feature for detecting and differentiating defects during subsequent processing stages. Maintaining color consistency is also a crucial prerequisite for 3D processing of the image data. Any disturbances in this spatially-resolved color texture, whether caused by lighting, lens, sensor, or variations in geometry of the primary image data, must be identified and eliminated. In our particular scenario, images are often affected by color shading, which manifests as shifts in chromaticity and brightness. Thus, it becomes essential to correct these systematic influences on the color textures.

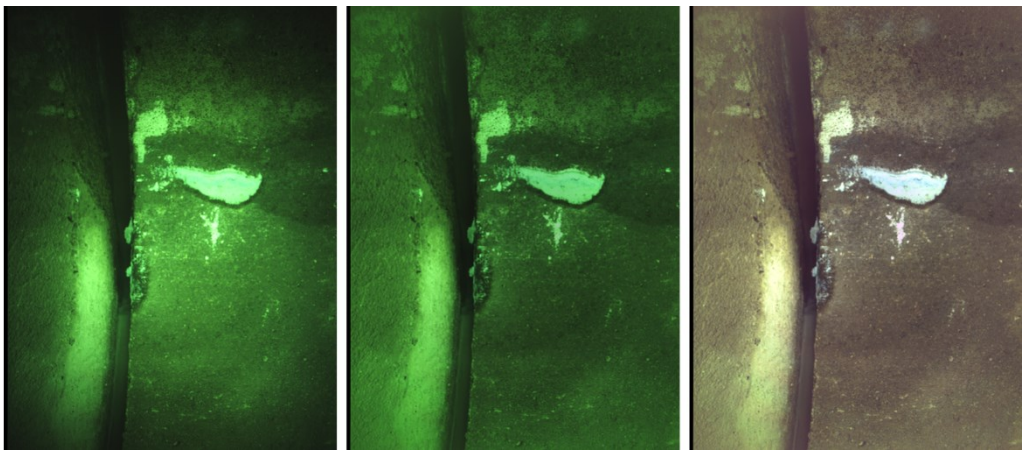

Figure 3: Illustration of a debayered color image with visible vignetting toward the periphery of the image (left). It is followed by the results of brightness shading correction (middle) and chromaticity correction (right).

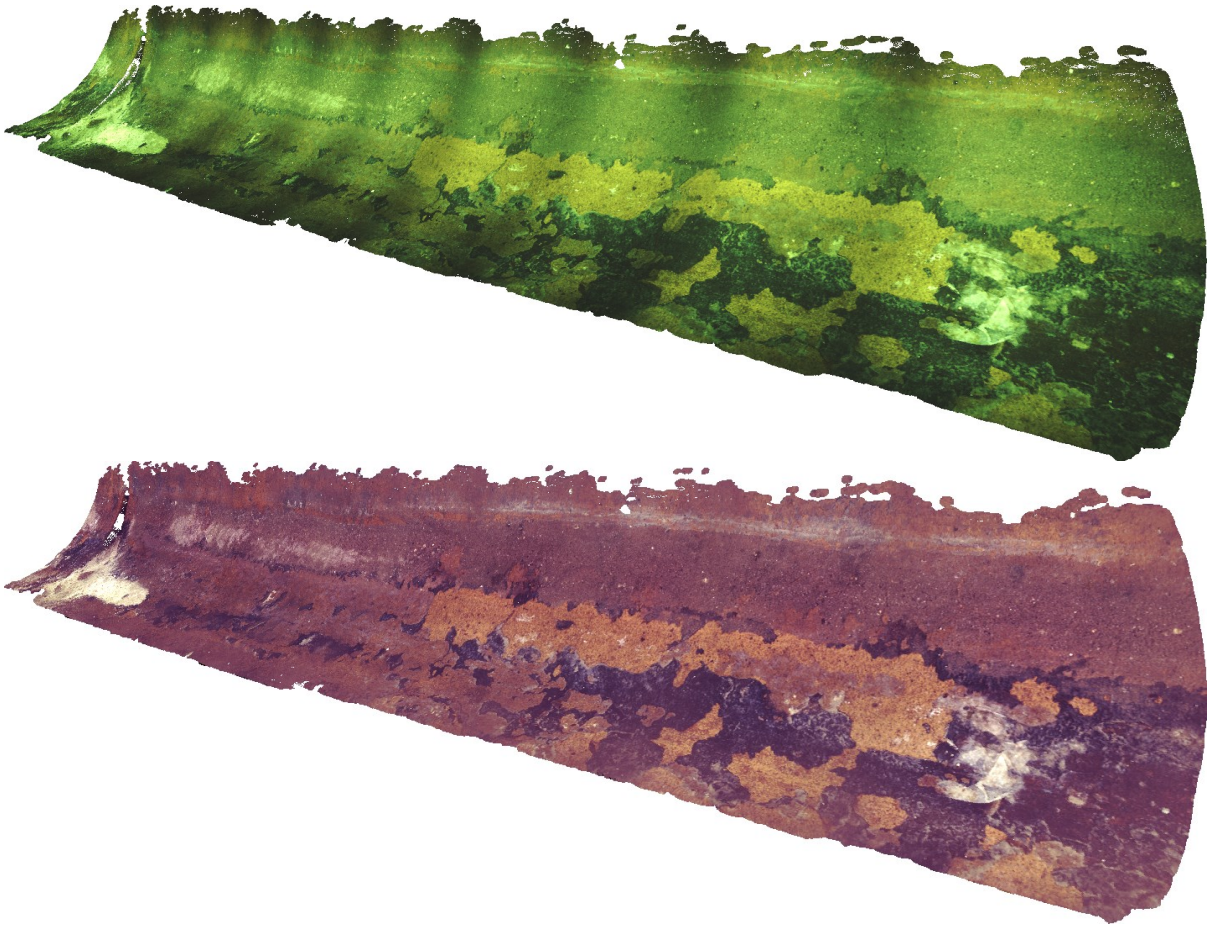

Figure 4: A DN200 pipe section in 3D with a greenish hue and shading (top). The same section after radiometrically applied color and shading corrections (bottom).

Applying conventional shading correction to the color image through a planar white reference is not feasible due to the variable distance between camera and scene objects, along with the complex shading influences, which often lead to artifacts like chromatic flares. To circumvent this issue, we employ a method where a reference light is estimated from images of the captured sewer section and color shading correction is applied using lightness and chromaticity features from the L*a*b* color space in all primary color channels. The efficacy of this correction can be appreciated from Figure 3 and Figure 4.

Beyond color correction, our process also mitigates motion blur that arises due to movement during image capture. This is achieved by leveraging prior knowledge of the cylindrical pipe geometry and utilizing a depth-graded unfolding method. In particular, we employ a parametric 1D - Wiener filter to enhance the sharpness of the color texture in a direct procedure of forward restoration.

3.2 Geometric system calibration and 3D reconstruction

We create a 3D point cloud using the state-of-the-art principle of triangulation. This process requires two matching points in the camera and projector image. These points, both representing the same location in the scene, allow us to project rays into 3D space using known geometric calibration parameters. The intersection of these rays reveals the desired 3D point. An important first step for these geometric evaluations is the calibration of each camera module.

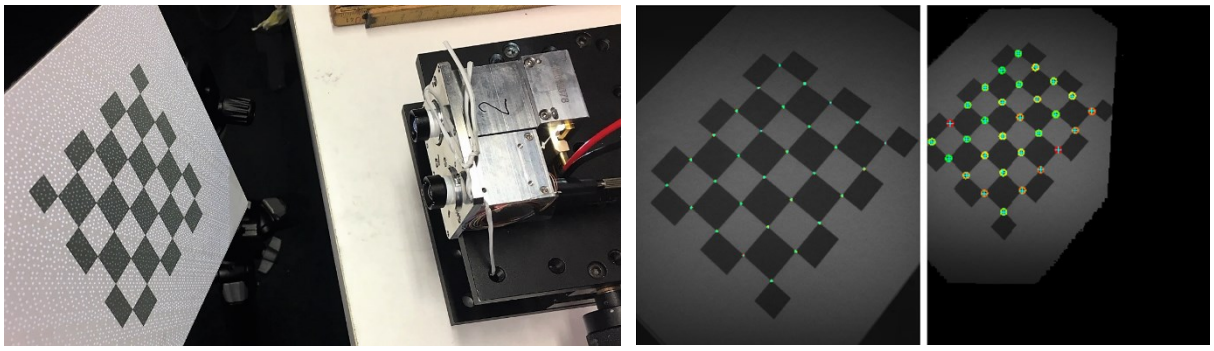

Figure 5: Calibration of the camera-projector modules is achieved intrinsically and extrinsically, utilizing several images of a calibration pattern (left) captured at varying distances and orientations. Calibration points detected in the camera and projector (right) are color-coded according to the re-projection error, serving as a visual indicator of calibration precision.

3.2.1 Geometric calibration

The imaging properties of the camera and the projector (which functions as an inverse camera) within each structured light module are approximated using a pinhole model. To address the notable lens distortion, we employ a Brown-Conrady distortion model. We captured between 15 to 20 calibration images for both the intrinsic and extrinsic calibration of the camera and projector. These images were obtained using a tripod-mounted target with a checkerboard pattern (Figure 5 left). The detection of the target, sub-pixel processing of calibration points, and parameter optimization were facilitated using the 3D-EasyCalib toolkit [14].

For intrinsic calibration, the camera matrix is established from images of a calibration target, its known world points, and corresponding image points. The calibration of both the projector and the extrinsic aspects of a camera-projector module need an additional step. Instead of a single image, we captured paired images of each target pose, one with the projected pattern off and ambient light on, and vice versa. The target images are processed similarly to the camera calibration. Pattern decoding provides the necessary geometric mapping between the image planes of the projector and the camera. Local homographies around each checkerboard corner are used to transfer calibration points between camera and projector images. The projector calibration matrix, as well as the projector's orientation and pose relative to the camera (extrinsics), are estimated using the same optimization process as for the intrinsic camera calibration. After establishing the intrinsic and extrinsic parameters of the camera and projector, we can triangulate corresponding image points that are identified using the procedures described in the following section.

3.2.2 Binary pattern

Our active snapshot-3D approach employs a binary coded spot pattern based on perfect submaps [15]. In these pseudo-random arrays, each sub-matrix of a fixed size, or codeword, appears exactly once. If a pattern built on perfect submaps covers the entire projector image, each projector pixel is uniquely encoded. This encoding is pivotal for solving the camera-projector correspondence problem. We opted for binary symbols as they allow independence from the spectral light interaction of detected objects. We derived the geometric properties of the pattern displayed in Figure 6 using the methodology from [13]. The generated pattern has a uniqueness window size of 6 by 6, a minimum Hamming distance of 3, and a minimum word weight of 4. The pattern is repeated horizontally and vertically to fill the entire projector image.

Figure 6: A binary pattern featuring a uniqueness window size of 6x6, utilized in the structured light modules. This pattern is repeated horizontally and vertically to cover the entire projector image.

3.2.3 Image decoding and 3D reconstruction

The computation of a 3D point cloud from a single camera image of the projected pattern is a multistep image processing procedure. Initially, a spot enhancement is performed to emphasize the spots and suppress the background, followed by local adaptive binarization. Next, the binary image is decoded. A regular grid of a consistent size is imposed on each camera pixel, and the binary value beneath each grid cell is read. This binary string, or codeword, is then cross-referenced in the coding table to resolve its position in the base pattern. This process establishes camera-projector correspondences. Finally, the 3D points are computed from the corresponding points in the respective camera and projector images using the linear triangulation method from [16]. A more comprehensive explanation of these steps, leading to the precise 3D point cloud, can be found in [13].

3.3 Mapping of a color texture to the depth image (RGB-D)

The process of capturing texture and pattern images involves a time-delayed operation executed by the same camera. Figure 7 shows the raw data processing steps needed to create a fused RGB-D image. Given the continuous motion of the cameras on the inspection robot, determining the offset between the 3D and texture images is essential for proper mapping. Since the pattern and texture images are distinct in their modalities (3D vs color), direct registration through correlation-based methods is not feasible. To overcome this, we capture an additional texture image, thereby creating a sequence comprising two texture images and one pattern image from a single camera burst. The spatial offset among these captured images is only a few millimeters, with all three images captured within 20 ms. Given that the inspection robot maintains a roughly constant forward motion within this narrow time window, we infer that the spatial position of the 3D pattern image is precisely at the midpoint between the two texture images. To determine rotation and translation between the two textures, we employ the methodology proposed by Tzimiropoulos et al. [17], which offers speed due to frequency domain correlations and robustness due to its global nature. Finally, the color and shading corrected texture, as described in Sec. 3.1, is transformed to overlap with the depth image, reconstructed as detailed in Sec. 3.2.

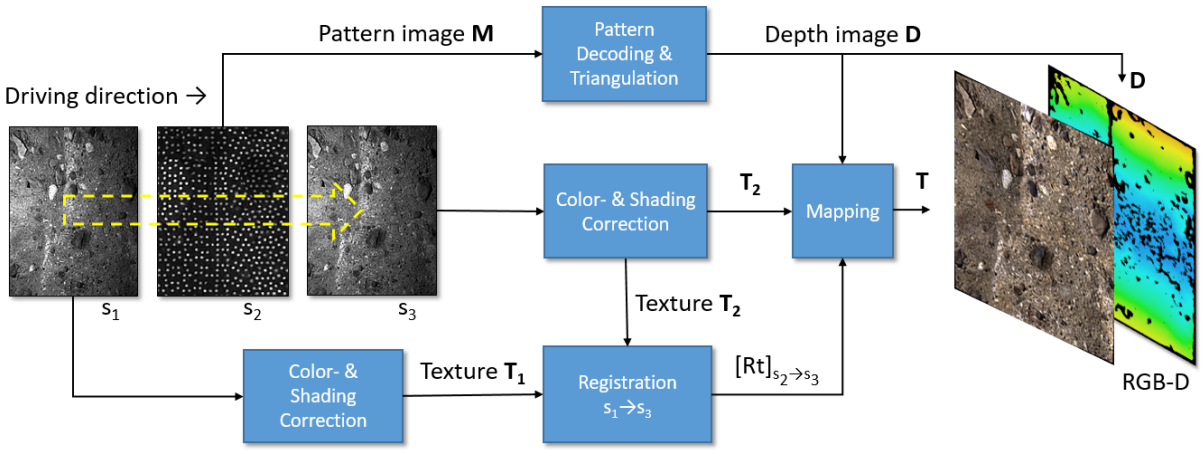

Figure 7: Processing pipeline for generating a color-textured depth image (RGB-D)

3.4 2D/3D-Registration and 3D data fusion of RGB-D-module data

The process of stitching RGB-D data primarily necessitates registration. This enables optimal transfer of texture and depth data of adjacent measurement areas for subsequent measurement data fusion. The feature-based 2D/3D registration procedure is illustrated in Figure 8. Ideally, we have available RGB-D data of two adjacent measurement regions with a 50% overlap. The first step involves finding and matching corresponding feature points [18], which are sought in the texture information associated with the depth data. To minimize the search area for matching, an initial estimate of transformation parameters is made, primarily based on the position information of an odometry module. On mobile robot platforms, a high 3D data rate often ensures that data points are already close to each other from image to image, thereby narrowing the search area for matching points. The list of candidate feature points is then gradually reduced according to various criteria. In the final filtering step, the essential matrix, which provides the rotation and the direction vector of the translation, is estimated while maintaining adherence to the epipolar condition. However, the calculation is still lacking the correct scaling, or magnitude, of the translation. To derive this, the 2D correspondences from the texture images are transformed into 3D correspondences using the depth maps and the known intrinsic camera parameters. This allows the Euclidean transformation to be resolved analytically in a clear and unambiguous manner. Several feature point determination procedures have been tested on real measurement data, with A-KAZE [19] features being selected due to low computational effort and robustness.

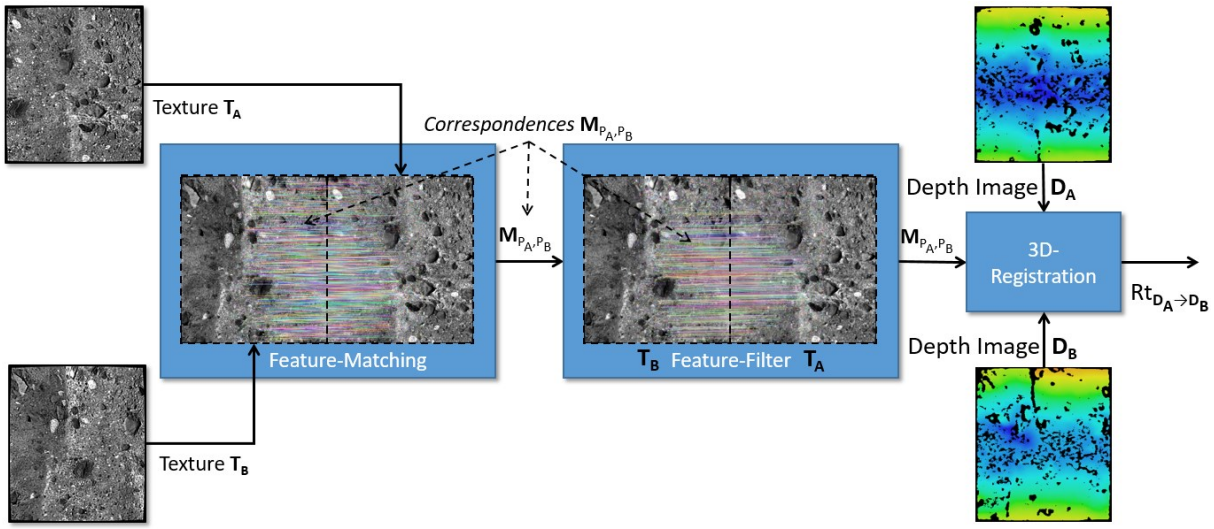

Figure 8: The processing pipeline of the feature-based, camera-related 2D/3D registration of sewer pipe interior sections.

Data fusion aims to close gaps and statistically reduce measurement uncertainty by summarizing corresponding measurement points of adjacent regions in overlap areas. A depth image can contain gaps caused by shadows, extreme spatial gradients of surface regions relative to the camera and projector, unfavorable size ratios of error object extent and pattern size, as well as other uncooperative imaging situations between projected pattern, object surface, and camera. Adjacent depth images may also contain gaps, usually located at different places due to their differing camera-projector perspectives. By merging the overlapping data, the gaps can largely be closed, and the measurement uncertainty in the already gapless areas can be reduced due to the multiple measurements. The starting point for data fusion is successful 2D/3D registration of the pictorial measurement areas as described in the previous section. Then all measurement areas can be transferred into a common coordinate system using Euclidean transformation. After outlier correction, the actual merge step takes place, implemented through

a block-based approach. All measurement points of the considered area are assigned to 2D raster blocks of a defined size. Quality-weighted thinning of the measurement points of each block occurs. To ensure minimum measurement point distances, the process is repeated for shifted raster blocks. The remaining points are then interpolated and mapped onto a regular grid of the target depth image. The end product is a fused RGB-D image as shown in Figure 9.

The process of combining all RGB-D images of each module from the captured section into a single 3D textured model is achieved using the global quadratic optimization described in [20]. The resultant 3D model, such as depicted in Figure 10, serves as the starting point for either automatic or manual multimodal damage classification of a new level.

4. CONCLUSION AND OUTLOOK FOR FUTURE WORK

In summary, this paper illustrates methods for a new level of multimodal acquisition of sewer pipe data using camera-projector modules based on a single-shot principle. We have elaborated on the optical setup and outlined the process of registering texture and depth information, as well as the stitching of measurement data, in the 3D acquisition of inner pipe surfaces. Both the hardware and the algorithmic aspects of this approach are innovative, and, as a result, fulfill the demanding requirements associated with objective channel inspection.

The sensor head, designed for versatility, can be adapted for usage across a range of sewer diameters, from 0.2 to 0.4 meters. Its robust 3D sensors tolerate off-centering within the sewer pipe, thereby enhancing its performance in variable conditions. The device has been engineered to capture data on-the-go, capable of functioning at a travel speed of up to 100 mm/s. It optically images the inner wall of the sewer in 3D, achieving a lateral resolution of 0.1 mm and a depth resolution of 0.2 mm. Furthermore, the sensor head records the surface texture in color, demonstrating its tolerance to the moisture present on the sewer inner walls, an inevitable feature of its operating environment.

Looking ahead, our research and development efforts will concentrate on further miniaturizing both the modules and the entire sensor head. By leveraging advancements in miniaturized cameras and projectors, particularly those incorporating diffractive optical elements, as proposed in [13], we aim to reduce the size of the entire sensor head to match that of the current single camera-projector module. Furthermore, we plan to optimize our processing pipeline by implementing it more directly on a System-on-Chip (SoC). We believe this will significantly reduce data transfer and offline processing time, ultimately improving the overall efficiency and usability of our system for sewer inspection and other potential applications.

ACKNOWLEDGMENTS

The results presented in this article are based on our work within the joint projects AuZuKa “Automatische Zustandsanalyse Kanalnetz durch virtuelle Begehung”, grant no. 13N13895 which is funded by the German Federal Ministry of Education and Research (BMBF).

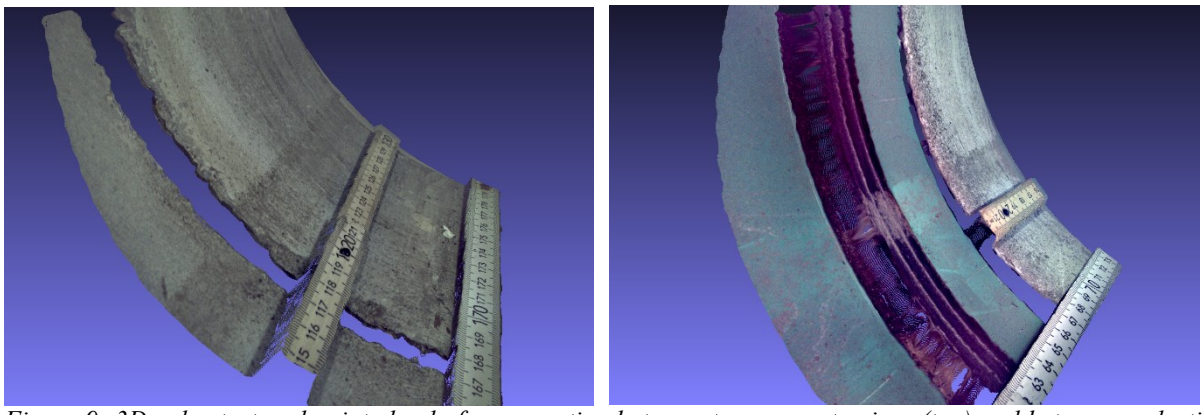

Figure 9: 3D color textured point cloud of a connection between two concrete pipes (top) and between a plastic and concrete pipe (bottom) as captured by a structured light module. The level of detail in both texture and 3D can be seen on the ruler and tape measure, as well as the pipes stacked at varying depths. Additional images and videos can be found at www.zbs-ilmenau.de/projekte/auzuka.

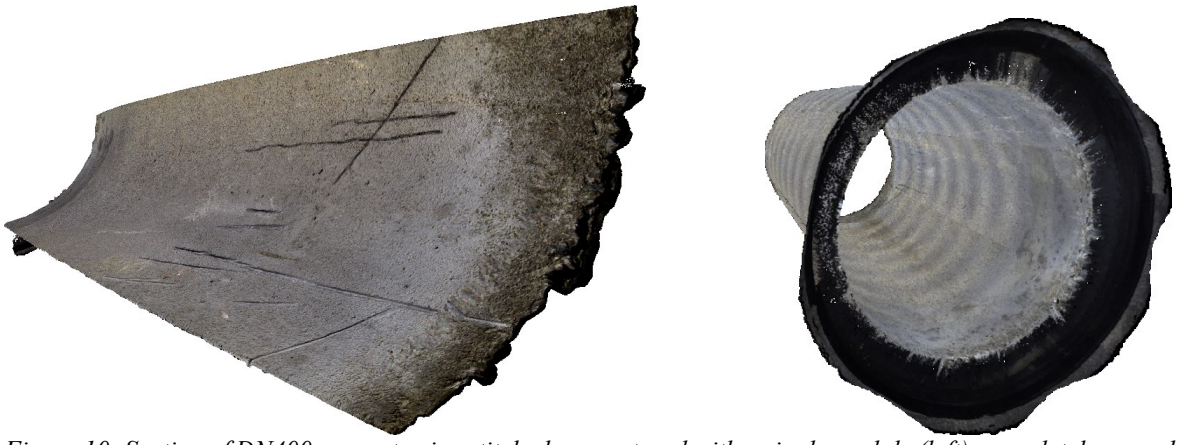

Figure 10: Section of DN400 concrete pipe stitched, as captured with a single module (left), completely assembled model of the pipe, from all modules (right). The images were taken in the laboratory of ZBS e. V.

REFERENCES

[1] J. Künzel, T. Werner, P. Eisert, J. Waschnewski, R. Möller, and R. Hilpert, "Automatic Analysis of Sewer Pipes Based on Unrolled Monocular Fisheye Images," *Proc. - 2018 IEEE Winter Conf. Appl. Comput. Vision, WACV 2018*, vol. 2018-Janua, no. March, pp. 2019–2027, 2018, doi: 10.1109/WACV.2018.00223.

[2] R. Orghidan, J. Salvi, and E. M. Mouaddib, "Accuracy estimation of a new omnidirectional 3D vision sensor," in *IEEE International Conference on Image Processing 2005*, 2005, pp. III–365, doi: 10.1109/ICIP.2005.1530404.

[3] N. Stanić, W. P. J. Van der Schoot, B. Kuijer, J. G. Langeveld, and F. H. L. R. Clemens, "Potential of laser scanning for assessing structural condition and physical roughness of concrete sewer pipes," *Proc. SPN7*, no. 2013, 2013.

[4] T. Wu, S. Lu, and Y. Tang, "An in-pipe internal defects inspection system based on the active stereo omnidirectional vision sensor," *2015 12th Int. Conf. Fuzzy Syst. Knowl. Discov. FSKD 2015*, pp. 2637–2641, 2016, doi: 10.1109/FSKD.2015.7382373.

[5] X. Chen, F. Zhou, X. Chen, and J. J. Yang, "Mobile visual detecting system with a catadioptric vision sensor in pipeline," *Optik (Stuttg).*, vol. 193, no. March, p. 162854, 2019, doi: 10.1016/j.ijleo.2019.05.060.

[6] Y. Zhang, R. Hartley, J. Mashford, L. Wang, and S. Burn, "Pipeline reconstruction from fisheye images," *19th Int. Conf. Cent. Eur. Comput. Graph. Vis. Comput. Vision, WSCG 2011 - Co-operation with EUROGRAPHICS, Full Pap. Proc.*, pp. 49–57, 2011.

[7] A. V. Reyes-Acosta, I. Lopez-Juarez, R. Osorio-Comparan, and G. Lefranc, “3D pipe reconstruction employing video information from mobile robots,” *Appl. Soft Comput. J.*, vol. 75, pp. 562–574, 2019, doi: 10.1016/j.asoc.2018.11.016.
[8] T. Y. Chuang and C. C. Sung, “Learning and SLAM based decision support platform for sewer inspection,” *Remote Sens.*, vol. 12, no. 6, 2020, doi: 10.3390/rs12060968.
[9] F. Chataigner *et al.*, “ARSI: An Aerial Robot for Sewer Inspection,” *Springer Tracts Adv. Robot.*, vol. 132, pp. 249–274, 2020, doi: 10.1007/978-3-030-22327-4_12.
[10] P. Huynh, R. Ross, A. Martchenko, and J. Devlin, “3D anomaly inspection system for sewer pipes using stereo vision and novel image processing,” *Proc. 2016 IEEE 11th Conf. Ind. Electron. Appl. ICIEA 2016*, pp. 988–993, 2016, doi: 10.1109/ICIEA.2016.7603726.
[11] C. Bellés and F. Pla, “A Kinect-Based System for 3D Reconstruction of Sewer Manholes,” *Comput. Civ. Infrastruct. Eng.*, vol. 30, no. 11, pp. 906–917, 2015, doi: 10.1111/mice.12107.
[12] M. Alzuhiri, R. Rathnakumar, Y. Liu, and Y. Deng, “A novel structured light based sensing and probabilistic diagnostic technique for pipe internal corrosion detection and localization,” *PHMSA R&D Forum*, 2020.
[13] D. Vehar, A. Hermerschmidt, R. Nestler, K. Franke, V. Zbs, and H. P. Ag, “Single-shot structured light with diffractive optic elements for real-time 3D imaging in collaborative logistic scenarios,” *Proc. SPIE Digit. Opt. Tehcnologies*, 2023.
[14] D. Vehar, R. Nestler, and K.-H. Franke, “3D-EasyCalib - Toolkit zur geometrischen Kalibrierung von Kameras und Robotern,” *22. Anwendungsbezogener Work. zur Erfassung, Model. Verarbeitung und Auswertung von 3D-Daten, 3D-NordOst*, no. December, pp. 15–26, 2019.
[15] R. Vandenhouten, A. Hermerschmidt, and R. Fiebelkorn, “Design and quality metrics of point patterns for coded structured light illumination with diffractive optical elements in optical 3D sensors,” *Digit. Opt. Technol. 2017*, vol. 10335, p. 1033518, 2017, doi: 10.1117/12.2270248.
[16] R. Hartley and A. Zisserman, *Multiple View Geometry in Computer Vision*, vol. 89. Cambridge University Press, 2004.
[17] G. Tzimropoulos, V. Argyriou, S. Zafeiriou, and T. Stathaki, “Robust FFT-based scale-invariant image registration with image gradients,” *IEEE Trans. Pattern Anal. Mach. Intell.*, vol. 32, no. 10, pp. 1899–1906, 2010, doi: 10.1109/TPAMI.2010.107.
[18] M. Muja and D. G. Lowe, “Fast approximate nearest neighbors with automatic algorithm configuration,” *VISAPP 2009 - Proc. 4th Int. Conf. Comput. Vis. Theory Appl.*, vol. 1, pp. 331–340, 2009, doi: 10.5220/0001787803310340.
[19] P. F. Alcantarilla, J. Nuevo, and A. Bartoli, “Fast explicit diffusion for accelerated features in nonlinear scale spaces,” *BMVC 2013 - Electron. Proc. Br. Mach. Vis. Conf. 2013*, no. December, 2013, doi: 10.5244/C.27.13.
[20] J. Künzel, D. Vehar, R. Nestler, K.-H. Franke, A. Hilsmann, and P. Eisert, “System for 3D Acquisition and 3D Reconstruction Using Structured Light for Sewer Line Inspection,” pp. 997–1006, 2023, doi: 10.5220/0011779900003417.

CONTACTS

Dipl.-Inf. Darko Vehar
E-Mail: darko.vehar@zbs-ilmenau.de
ORCID: https://orcid.org/0009-0006-3230-1934

Dr.-Ing. Rico Nestler
E-Mail: rico.nestler@zbs-ilmenau.de
ORCID: https://orcid.org/0009-0002-6551-6692